Genital organ-associated lymphoid tissues arranged in a ring in the mucosa of cow vaginal vestibules

Tsolmon Chuluunbaatar[1,2], Osamu Ichii[1,3], Md. Abdul Masum[4], Takashi Namba[1], Md. Rashedul Islam[1,5], Yuki Otani[1], Yaser Hosny Ali Elewa[1,6], Yasuhiro Kon[1*]

1. Laboratory of Anatomy, Department of Basic Veterinary Sciences, Faculty of Veterinary Medicine, Hokkaido University, Hokkaido 060-0818, Japan
2. Department of Basic Science of Veterinary Medicine, School of Veterinary Medicine, Mongolian University of Life Science, Ulaanbaatar 17024, Mongolia
3. Laboratory of Agrobiomedical Science, Faculty of Agriculture, Hokkaido University, Hokkaido 060-8589, Japan
4. Department of Anatomy, Histology, and Physiology, Faculty of Animal Science and Veterinary Medicine, Sher-e-Bangla Agricultural University, Dhaka 1207, Bangladesh
5. Department of Surgery and Theriogenology, Faculty of Animal Science and Veterinary Medicine, Sher-e-Bangla Agricultural University, Dhaka 1207, Bangladesh
6. Department of Histology, Faculty of Veterinary Medicine, Zagazig University, Zagazig 44519, Egypt

* Corresponding author: Yasuhiro Kon, DVM, PhD

Laboratory of Anatomy, Department of Basic Veterinary Sciences, Faculty of Veterinary Medicine, Hokkaido University, Kita 18-Nishi 9, Kita-ku, 060-0818 Sapporo, JAPAN

Tel/Fax: +81-11-706-5188, E-mail: y-kon@vetmed.hokudai.ac.jp

Abstract

Female reproductive tracts are equipped with local and mucosal immune systems; however, structural information remains unclear for farm animals. In this study, the mucosa-associated lymphoid tissue-like structures in cow reproductive tracts were described. Vaginal vestibule (VV) and external parts of the genital organ, including the clitoris and vulva, were morphologically analyzed. Whole-mount specimens revealed several hematoxylin-positive spots arranged in a ring in the mucosa. Histologically, these spots were aggregated immune cells and defined as genital organ-associated lymphoid tissues (GOALTs). GOALTs were composed of lymphatic follicles (LFs) or diffuse lymphoid tissues (DLTs) at different depths of lamina propria. LFs frequently contained germinal centers. Scattered lymphocytes occupied the border area between follicles and epithelium, whereas DLTs had indefinite shapes. GOALTs contained immune cells and high endothelial venules. B cells were dominant both in LFs and DLTs. Abundant collagenous fibers were stretched across VV lamina propria, whereas reticular fibers were primarily observed in the DLT rather than LF. The epithelium covering of GOALTs was partially or fully disrupted by the invasion of immune cells toward the VV lumen. These findings suggest GOALTs function as a “genital lymphoid ring” as in Waldeyer’s pharyngeal ring and act as immunological gate systems in cow reproductive tracts.

Keywords

Cow; Genital organ associated lymphoid tissue; Lymphoid ring; Lymphatic follicle; Diffuse lymphoid tissue

Introduction

The mucosa-associated lymphoid tissue (MALT) is a local immune system beneath the mucosal epithelium (Kenneth Murphy, 2017; Lanzkowsky et al., 2016). MALTs are located in systemic organs that directly contact the outer environment, including alimentary tracts, salivary gland ducts, conjunctiva, nasopharynx, and respiratory tracts (Forchielli and Walker, 2005; Kenneth Murphy, 2017; Knop and Knop, 2011; Kracke et al., 1997; Kuper et al., 1992; Moyron-Quiroz et al., 2004; Nair and Schroeder, 1986; Randall, 2010). Gut-associated lymphoid tissue (GALT) is a well-known MALT and also known as Peyer's patches (Forchielli and Walker, 2005). In the oropharynx, there are ring-shaped localized MALTs, including the lingual, palatine, and pharyngeal areas and the tubal tonsils (Hellings et al., 2000). Waldeyer's pharyngeal ring is the sentinel for the oral, nasal, and auditory tracts toward to the pharynx and basically functions in antibody production to protect against regular environmental antigens (Liebler-Tenorio et al., 2006; Manesse et al., 1998).

MALTs mainly consist of lymphoid tissues (LTs) with two types of morphology. Briefly, the lamina propria of several MALT-forming organs exhibit diffused arrangement of immune cells, and this type is called diffuse LT (DLT). However, in several MALTs, the accumulation of immune cells is separated by connective tissue from surrounding tissues,

63 and these are called lymphatic follicles (LFs) or lymph nodules (Wojciech and Ross, 2020).
64 Furthermore, the MALT is composed of B cells, $CD4^+$, or $CD8^+$ T-cells, antigen-presenting
65 cells (APCs), macrophages, and occasionally, mast cells and eosinophils. Each cell is
66 well-situated to initiate an immune reaction when encountering antigens passing through
67 the mucosal epithelium (Cesta, 2006).

68 Mammalian female reproductive tracts are also in close contact with the outer
69 environment and maintain innate and adaptive immune systems constructed by the
70 epithelial barrier, the production of antimicrobial agents, cytokines secreted by the
71 epithelial cells, and the innate immune cells (Hickey et al., 2011; Mair et al., 2014).
72 Importantly, the reproductive tracts of humans or other animal species contain MALT with
73 species- or disease-specific variations in morphology. A series of studies on LT have
74 recently been pursued in some female genital tracts, including the vaginal vestibule (VV),
75 vagina, cervix, uterus, and oviducts in non-human primates, pigs, and cows to evaluate the
76 effects of drug administration or mucosal vaccination (Blazquez et al., 1987a; Kathrine and
77 Steen, 2011; Lehner et al., 1995). Specifically, the guiana dolphin (*Sotalia guianensis*)
78 exhibited aggregations of LFs in the lamina propria of their uterine(Silva et al., 2016).
79 Importantly, healthy female mice did not have MALT in their reproductive tracts, but they
80 exhibited a MALT-like structure in their vaginal mucosa after receiving intravaginal
81 immunization with a specific peptide (Wang et al., 2015). Furthermore, locally organized
82 MALT in the VV observed in patients with provoked vulvodynia compared with healthy
83 women, indicated the MALT emerged because of the local alternation of VV
84 morpho-function (Liebler-Tenorio et al., 2006; Tommola et al., 2015).

The reproductive management of animals is crucial in veterinary medicine. In cattle, gross anatomically and functionally, MALT in the alimentary and respiratory tract has been well-investigated in several studies (Anderson et al., 1986; Manesse et al., 1998; Parsons et al., 1989). Briefly, several types of MALTs were established according to their anatomical localization, including GALTs, conjunctiva-associated LTs, and bronchus-associated LTs (Anderson et al., 1986; Chodosh et al., 1998). Importantly, epithelium-associated LF aggregations were suggested throughout the reproductive tracts in cattle, including the VV (Blazquez et al., 1987a). The LF aggregations located in the lamina propria of the clitoris and VV could play an important role in immune induction sites because of their appearance during infection with cow reproductive tract pathogens (Blazquez et al., 1987b; Wang et al., 2011); however, structural information on reproductive tract-associated MALTs, in particular their localizations, morphological types, and cellular composition, has received limited attention.

In the present study, we found a MALT-like structure arranged in a ring around the cow VV, and the stratified epithelium covering the LT was partially or completely disrupted, which permitted direct passage of immune cells and erythrocytes into the intraluminal space. We named these LTs the “genital lymphoid ring” and discussed the similarities with Waldeyer’s pharyngeal ring, which acts as an immunological gate.

Materials and methods

Animal and sample preparation

106 Animal experimentation procedures were approved by the Institutional Animal Care and
107 Use Committee of the Faculty of Veterinary Medicine, Hokkaido University (approval no.
108 19-0097). Investigators adhered to the Guidelines for the Care and Use of Laboratory
109 Animals of Hokkaido University, Faculty of Veterinary Medicine. All animal experimental
110 protocols were approved by the Association for Assessment and Accreditation of
111 Laboratory Animal Care International. Holstein breed, normal non-pregnant cows (total n =
112 8, over 2-year-old) were sedated with xylazine (3.0 mg/kg body weight) through an
113 intramuscular route followed by general anesthesia with pentobarbital sodium (500 mg/kg
114 body weight) via the intravascular route (Supplemental table 1). The cows were sacrificed
115 by intravenous administration of a saturated potassium chloride solution of at least 0.1
116 mL/kg body weight. Then, the jugular vein was exsanguinated. After euthanasia, female
117 genital organs were obtained, and the vagina, VV, and EPGOs, including the clitoris and
118 vulva were separated. They were immediately fixed in 10% neutral buffered formalin for
119 more than 7 d. These specimens were dissected using scissors at the dorsal commissure
120 along the median line of the vulva to the vagina.
121

122 *Whole-mount observation*

123 Separated genital organs were pinned flat, with the mucosa uppermost, and immersed in
124 Mayer's hematoxylin for approximately 10 min (examining at 3–4 min intervals) to
125 visualize LTs. LTs were then visible as small navy-blue spots. To decrease the intensity of

126 the staining background, specimens were rinsed in 70% alcohol containing 1%
127 hydrochloric acid.

128 Counting of hematoxylin-positive spots was performed for the VV and EPGOs.
129 Flattened VV and EPGOs were divided into six regions (**Fig. 1**). Briefly, we divided the
130 VV and EPGOs into two equal regions (cranial and caudal) along the horizontal line (the
131 length of the external urethral orifice to the ventral commissure was divided into two equal
132 lengths). Then, the cranial and caudal regions were subdivided by two vertical lines into
133 three equal subregions. The external urethral orifice was located at the center of the cranial
134 median region (**Fig 1, region II**), and the clitoris was located at the center of the caudal
135 median region (**Fig. 1, region V**). Each area was measured using ImageJ (National
136 Institutes of Health; MD, Bethesda, USA) after taking photos with a DMC-FX3799 device
137 (Panasonic; Osaka, Japan). The number of hematoxylin-positive spots was counted, and
138 their density in each region was calculated.
139

140 *Histoplanimetry*

141 The VV of each cow was cut into more than 15 pieces according to their size. Then,
142 whole-mount specimens with hematoxylin were embedded into paraffin and cut to a
143 thickness of 5 μm. Sections were stained with hematoxylin and eosin (H&E) or PSR for
144 histological analysis. Stained sections were scanned with a NanoZoomer 2.0 RS virtual
145 slide scanner (Hamamatsu Photonics; Shizuoka, Japan). Histological images for
146 microscopic examinations were observed using a model BZ-X710 microscope (Keyence;

147 Osaka, Japan). The number of LFs and DLTs was counted after H&E staining. This
148 measurement was performed for more than 120 sections of eight cows. We also
149 characterized the LFs according to their localization (isolated, migrating, bordering) and the
150 DLTs according to their shape (oval, c-shaped, triangle, amorphous), and their
151 appearance % was calculated.
152

153 *Immunohistochemistry (IHC)*

154 IHC was performed to evaluate the presence of B-cells (CD20), T-cells (CD3),
155 macrophages (IBA1), APCs (MHCII), high endothelial venules (PNAd), and tight junctions
156 (Occludin). The staining conditions of each antibody are listed in Supplementary table 2. In
157 brief, sections were deparaffinized and incubated in 10 mM citrate buffer (pH 6.0) or
158 Tris-HCl buffer (pH 9.0) for 15 min at 110 °C. Thereafter, slides were submerged in
159 methanol containing 0.3% H_2O_2 for 20 min at 20–22 °C and blocked with normal goat
160 serum (SABPO kit, Nichirei Bioscience; Tokyo, Japan) for 1 h at room temperature.
161 Sections were incubated with primary antibody overnight at 4 °C. After rinsing in
162 phosphate-buffered saline (PBS), sections were incubated with biotinylated secondary
163 antibody (goat anti-rabbit or goat anti-rat) for 30 min and streptavidin-horseradish
164 peroxidase (Nichirei Bioscience) for 30 min at room temperature. To develop the color,
165 sections were incubated in a 3,3'-diaminobenzidine tetrahydrochloride‑hydrogen peroxide
166 solution for 4 min. Finally, the sections were counterstained with hematoxylin and

dehydrated with ascending grades of alcohols. After washing with PBS, the sections were mounted and examined using a BZ-X710 microscope.

Next, we performed the histoplanimetrical analysis of LTs using the IHC sections for CD20, CD3, IBA1, and MHCII. More than 10 LFs and DLTs were examined. Firstly, total area of LFs or DLTs and the positive reaction area for each marker were measured, and percentage of the latter to the former was calculated.

Electron microscopy

For SEM, small pieces of VV were treated with tannic acid and post-fixed with 1% OsO_4 (osmium tetroxide) for 1 h. Then, the specimens were dehydrated in ascending grades of alcohol, immersed in 3-methylbutyl acetate, and dried with the HCP-2 critical point dryer (Hitachi; Tokyo, Japan). The specimens were then observed under an S-4100 scanning electron microscope (Hitachi).

Statistical analyses

The results are expressed as the mean ± standard error (SE). Multiple comparisons were performed using the Kruskal–Wallis test followed by the Scheffé method when a significant difference was observed ($P < 0.01$).

Results

LT found in the VV and external parts of genital organs (EPGO) mucosa of cows

We investigated the mucosa of the vagina and VV extending from the external urethral orifice to the vulva, and the vulva along with the pudendal labia and clitoris were also examined as EPGOs (**Supplemental figure 1**). Whole-mount specimens were visualized for hematoxylin-positive spots in the examined mucosae; in particular, we focused on VV and EPGOs because these areas are close to the outer environment and have contact with urine and feces. All examined cows had numerous hematoxylin-positive spots in the mucosal surface of the VV and EPGOs, and these spots were distributed at an approximately 1 cm distance from the boundary of the un-haired pudendal labia (**Fig. 1A, B**). Furthermore, 37.5% of examined cows showed these spots in EPGOs (three of eight cows), especially in the area close to the clitoris (**Fig. 1C**). Then, these spots were histologically identified as LT (**Fig. 1D**), and classified as genital organ-associated LTs (GOALTs). They were further investigated in subsequent experiments.

We also examined the localizations of GOALTs by dividing the VV and EPGOs into six regions (**Fig. 1E**). During the histometry of the density of GOALT spots for the six examined regions, region II and V, located along the ventral median line of the VV, including the external urethral orifice, clitoris, and ventral commissure of the labia, tended to exhibit a higher density without significance (**Fig. 1F**). These results indicated that GOALTs were distributed in the mucosa of the VV and EPGOs in a ring shape; therefore, we denoted the GOALT distributions as a "genital lymphoid ring," based on "Waldeyer's lymphoid pharyngeal ring." In subsequent analysis, we focused on VV mucosa.

Histology of GOALTs found in the cow VV mucosa

The histological observation was performed in the VV. The mucosa was covered by non-keratinized and stratified squamous epithelium (**Fig. 2**). The GOALTs were mainly localized in the lamina propria in the VV. Importantly, regarding the LT structures, two different types of GOALTs were found in the VV; LF (**Fig. 2A-D**) and DLT (**Fig. 2E-H**). For LF, three types were primarily observed in the VV mucosa based on their morphology. First, several LFs were localized in the deep portion of the lamina propria and fully surrounded by connective tissues. In this type, the VV epithelium completely maintained the structure (**Fig. 2A**). Second, scattered lymphocytes were observed between the LF and VV epithelium, and these lymphocytes were also thoroughly or partially observed within the VV epithelium structure (**Fig. 2B**). Third, LF directly faced the VV lumen, and the VV epithelium was occupied by lymphocytes (**Fig. 2C**). Further, most of the LFs were solitarily, but paired LFs were also noticed (**Fig. 2D**). Additionally, several shapes of DLTs were observed, such as triangle-, C-shaped-, amorphous-, and oval-types **(Fig. 2E-H)**.

In the histometry of the VV mucosa, LF- and DLT-types accounted for 35% and 65%, respectively (**Fig. 2I**). Furthermore, as a result of morphometry according to the LF localization, migrating-, isolated-, and bordering-types accounted for 51%, 37%, and 12%, respectively (**Fig. 2J**). Finally, for the DLT shapes, amorphous-, oval-, C-shaped-, and triangle-types accounted for 57%, 30%, 9%, and 4%, respectively (**Fig. 2K**).

Cell composition of GOALTs in the cow VV mucosa

230 Regarding LFs of the GOALT in the VV mucosa, numerous $CD20^+$ B cells were found,
231 and the germinal center and an area between the LF and VV epithelium were located (**Fig.**
232 **3A**). Further, $CD3^+$ T cells were diffusely distributed in LFs, including the germinal center,
233 and tended to mainly localize along the border area between the LF and VV epithelium
234 (**Fig. 3B**). $IBA1^+$ macrophages and $MHCII^+$ APCs were similar in localization and were
235 located in the germinal center and the border area between the LF and VV epithelium; the
236 former was also localized in the VV epithelium (**Fig. 3C, D**). Next, $PNAd^+$ high endothelial
237 venules were localized around the LFs and in the border area between the LF and VV
238 epithelium (**Fig. 3E**). In agreement with histological observations, the percentage of B cells
239 was statistically significantly higher in LFs than the percentage of T cells, macrophages,
240 and APCs ($P < 0.01$, **Fig. 3F**).
241 In the DLT, B cells, T cells, macrophages, APCs, and high endothelial venules were
242 dispersed diffusely (**Fig. 4A-E**). Similar to LFs, DLTs had a statistically significantly
243 higher percentage of B cells than that of other examined immune cells ($P < 0.01$, **Fig. 4F**).
244
245 *Histology of epithelial cells covering the GOALT in the cow VV mucosa*
246 Histologically, the VV mucosa was covered by stratified epithelial cells, wherein the basal
247 layer was smaller with narrow cytoplasm, and their nuclei were located close to one another
248 (**Fig. 5A**). Follicular epithelial cells found in MALTs were not identified. Importantly, in
249 several LTs, the thickness of the epithelium gradually became smaller towards the
250 epithelium covering LTs (**Fig. 5A**). Furthermore, the epithelium covering LTs showed
251 complete destruction of each junction of epithelial cell with numerous lymphocytes and

252 erythrocytes, and several epithelial cells peeled off and created a large junctional gap,
253 which permitted direct passage of immune cells into the intraluminal space of the VV (**Fig.**
254 **5B**). Occludin^{+} reactions were observed in the intercellular region of the epithelial cells, but
255 these were unclear in the epithelium covering LTs (**Fig. 5C, D**).

256 Next, picrosirius red (PSR) staining revealed the developed connective tissue fibers in
257 the lamina propria of the VV mucosa. Under polarized light observation, well-developed
258 collagen fibers were visualized as bright orange to red, whereas thinner reticular fibers
259 appeared yellow to green (**Fig. 5E**). In GOALTs, the DLT-types contained abundant
260 collagen and reticular fibers, but they were scarce in the LF-type (**Fig. 5E**). The VV
261 mucosa exhibited well-developed collagen and reticular fibers beneath the epithelium (**Fig.**
262 **5F**), but they were obscure in the LF (**Fig. 5G**).

263

264 *Ultrastructure of surface of LT in the VV*

265 Next, we observed the GOALT surface in the VV mucosa (**Fig. 6**). Whole-mount staining
266 with hematoxylin revealed the GOALTs as spots (**Fig. 6A**). Using scanning electron
267 microscopy (SEM), the epithelium covering GOALTs was found to partially lack in several
268 areas (**Fig. 6B**). Briefly, at these regions, several polygonal-shaped epithelial cells were
269 peeled off, and lymphocytes appeared to be directly exposed to the intraluminal space
270 through the hole (**Fig. 6C, D**). **Figure 6E** shows the large sized, dome-shaped LF covered
271 by the VV epithelium, which was approximately 350–480 μm in a diameter. Several
272 differently sized destroyed areas of the epithelium fused with each other and formed a
273 complicated cleft. From the inside of the GOALT, erythrocytes were also exposed directly

to the intraluminal space (**Fig. 6F, G**). Additionally, small protrusions occurred that appeared to be lymphocytes pushed up to the surface of the epithelium (**Fig. 6F, G**). Some connective tissue fibers were also observed inside of the GOALT and opened to the lumen (**Fig. 6G**). Summary of general quantitative data shown in **supplemental table 3**.

Discussion

This study clarified the morphological characteristics of GOALTs found in the VV and EPGOs of the cow. In cows, the VV extends from the external urethral orifice to the ventral commissure of the labia and is composed of the caudal part of the reproductive and/or urinary system, localized ventral to the anus, with a length of approximately 7–11 cm (Budras and E.Habel, 2003; Konig and Liebich, 2007). The LTs in the bovine VV were previously suggested in cows (Blazquez et al., 1987b; Cole, 1930; Hammond, 1927), but detailed morphological information was lacking. The high abundance of LTs along the VV may relate to increased antigenic stimulation in this region. In the present study, the ventral median region (II and V containing EPGOs) of the VV and EPGOs tended to have a greater number of GOALTs than other areas. We considered that the developed GOALTs in this area reflected the possibility of high exposure to antigenic substances, such as urine or feces, because of the anatomical localization of the VV. These relationships between antigenic challenge and the localizations of LTs are compatible with statements regarding the amount and type of MALTs being partially dependent on the antigenic challenge (Chuluunbaatar et al., 2020; Jericho et al., 1971; Pollard and Sharon, 1970). Additionally,

296 the age of the cow appeared to be a factor influencing the amount of LT, and the VV of
297 adult cows contained a significantly higher number of LTs than 6–8-week-old calves
298 (Blazquez et al., 1987a).

299 GOALTs were morphologically divided into LFs and DLTs, and the latter was
300 dominant in the VV. LFs were usually dispersed solitarily in a random manner throughout
301 the mucosa of the VV or EPGOs. Most LFs had a germinal center, which initiated a series
302 of events that included lymphocyte activation and proliferation, plasma cell differentiation,
303 and antibody production. Mitotic patterns were frequently seen in the germinal center,
304 indicating that new lymphocytes were proliferating *in situ* (Wojciech and Ross, 2020).
305 Although our histological data showed different morphology of LFs, the dominant was the
306 migrating-type, and sectioning of LFs also could have affected their shape observed during
307 microscopy. SEM analysis revealed both an epithelium-covered area (isolated-type) and
308 non-covered area (migrating-, bordering-type) in the same LF. Furthermore,
309 three-dimensional analysis of LFs could clarify their fine structure.

310 DLTs typically do not have a distinct border with surrounding tissues, rather have an
311 amorphous shape and are tactically localized to intercept antigens and initiate an immune
312 response. In general, after contact with antigen, lymphocytes located in the LT move to
313 regional lymph nodes, where they can sustain proliferation and differentiation. Then, the
314 progenies of these cells return to the lamina propria as B and T lymphocytes with effector
315 functions. Therefore, combined localization of LFs and DLTs in the VV or EPGO mucosa
316 could act as a protector of the reproductive tract against pathogenic substances.
317 Furthermore, our histological data showed the different morphology of LFs; the dominant

318 amorphous-type, with variation in the morphology of DLT that might reflect the difference
319 in the activation phase of GOALTs.

320 Subsequently, the percentage of the positive area for the immune cells calculated in
321 GOALT and both DLTs and LFs was dominated by B cells in comparison with T cells,
322 macrophages, and APCs. This was an expected finding, which is in agreement with other
323 research data, including those for the mice spleen, Peyer's patches, isolated LFs, and cow
324 and rabbit GALT (Hamada et al., 2002; Komban et al., 2019; Parsons et al., 1989;
325 Schneider et al., 2001).

326 The cell components of the cow GOALT showed close similarities to those of other
327 MALTs (GALT and Waldeyer's pharyngeal ring); however, the cell distribution was
328 generally solitarily and randomly localized within the VV and EPGOs (Owen and Jones,
329 1974). One of the most important cell components in MALTs is the APC. In this study,
330 APCs were found around the DLT and LF in different regions of the mucosal epithelium,
331 such as the germinal center, mantle zone, submucosa, and middle layers of stratified
332 squamous epithelium of the VV. These strategically positioned localizations might play
333 important roles in the initiation of immune reactions and maintenance of peripheral
334 tolerance. Therefore, various types of APCs in the LTs have different ways to take up
335 antigens from the lumen, including endocytosis, phagocytosis, or transcytosis (Zhang et al.,
336 2007). Although, in this study, the epithelium that covered GOALTs was thinner than areas
337 not covering GOALTs, and in some areas, the epithelium structure was completely lost, and
338 LT and the intraluminal area were directly bordered without any edge. This formation of
339 LT allows direct passage of antigens to the LT and immune cells from the intraluminal area.

As described in the literature (Brandtzaeg et al., 2008), MALT is divided into two specific types, an organized MALT delimited by organized collagen fiber tissue and a disorganized or diffuse MALT, comprising populations of lymphocytes from the lamina propria and the base of the epithelial lining, which are consistent with LFs and DLTs. LFs located in the conjunctiva have a lenticular shape, and occasionally around this area, the basement membrane is mostly discontinuous, and the epithelium is thinner (Crespo-Moral et al., 2020). We classified DLTs by shape, and each shape might reflect the different LT activity in the VV mucosa.

We studied the normal histomorphology of the GOALT, and unfortunately, the phase of the estrus cycle was impossible to identify in the examined cows. Importantly, the immune system in the female reproductive tract is precisely influenced and regulated by sex steroid hormones, estradiol and progesterone, which are produced in cyclic variations by the ovary during the estrus cycles. Throughout the estrus cycle, immune cells are present in considerable numbers and inconsistently distributed in the stromal layer and the epithelium of the female reproductive tract (Bulmer and Earl, 1987; Hunt, 1994). Moreover, the epithelial barrier of the reproductive tract, which includes various tight junction conditions, provides immune protection by maintaining a strong physical barrier, transferring antibodies to the mucosa, producing antibacterial composites, and recruiting immune cells, all of which are influenced by hormones (Russell and Mestecky, 2002)(Ochiel et al., 2008). Additionally, the various shapes of GOALTs found in the VV and EPGOs may be affected by different phases of the estrus cycle. A limitation of this study was the small sample size available to identify whether or not the estrus cycle

362 influences the amount of GOALT in the VV in cows. Further study is needed to clarify the
363 GOALT amount at every stage of the estrous cycle.

364 In summary, this study morphologically and histologically evaluated GOALTs in the
365 VV and EPGOs of cows, which constituted a "genital lymphoid ring." Regarding GOALT
366 morphology (**Fig. 7**), the mucosal epithelium covering DLTs and LFs was partially or
367 completely demolished, making a direct passage for immune cells to reach the luminal side.
368 The clarification of the morphology of GOALTs in cow genital tracts would contribute to
369 our understanding of its immune-associated function, the pathogenesis of diseases, and the
370 development of therapeutic strategy by applying mucosal vaccinations targeting GOALTs
371 in farm animals.

372

373 **Declarations of competing interest**

374 The authors declare that they have no known competing financial interest or personal
375 relationships that could have influenced in any way the work reported in this paper.

376

377 **Acknowledgments**

378 This work was supported by WISE KAKENHI and JSPS KAKENHI (Grant No.:
379 19H03113).

380

381 **Author Contributions**

YK and OI supervised the findings of this study. MAM, YHAE, TENA, TANA, MRI, and YO provided critical feedback and helped shape the research, analysis, and manuscript. TC, OI, and YK analyzed data and wrote the paper.

References

Anderson, M.L., Moore, P.F., Hyde, D.M., Dungworth, D.L., 1986. Bronchus associated lymphoid tissue in the lungs of cattle: relationship to age. Res. Vet. Sci. 41, 211–220.

Blazquez, N.B., Batten, E.H., Long, S.E., Perry, G.C., 1987a. Amount and distribution of vestibular-associated lymphoid tissue in calves and adult cows. Res. Vet. Sci. 43, 239–242.

Blazquez, N.B., Batten, E.H., Long, S.E., Perry, G.C., 1987b. Histology and histochemistry of the bovine reproductive tract caudal to the cervix part I. The vestibule and associated glands. Br. Vet. J. 143, 328–337.

Brandtzaeg, P., Kiyono, H., Pabst, R., Russell, M.W., 2008. Terminology: Nomenclature of mucosa-associated lymphoid tissue. Mucosal Immunol. 1, 31–37.

Budras, K.-D., E.Habel, R., 2003. Bovine Anatomy, 1st ed. Schlutersche, Hannover.

Bulmer, J.N., Earl, U., 1987. The expression of class II MHC gene products by fallopian tube epithelium in pregnancy and throughout the menstrual cycle. Immunology 61, 207–213.

Cesta, M.F., 2006. Normal structure, function, and fistology of mucosa-associated

402 lymphoid tissue. Toxicol. Pathol. 34, 599–608.

403 Chodosh, J., Nordquist, R.E., Kennedy, R.C., 1998. Comparative anatomy of mammalian
404 conjunctival lymphoid tissue: A putative mucosal immune site. Dev. Comp. Immunol.
405 22, 621–630.

406 Chuluunbaatar, T., Ichii, O., Nakamura, T., Irie, T., Namba, T., Islam, M.R., Otani, Y.,
407 Masum, M.A., Okamatsu-Ogura, Y., Elewa, Y.H.A., Kon, Y., 2020. Unique running
408 pattern and mucosal morphology found in the colon of cotton rats. Front. Physiol. 11.

409 Cole, H.H., 1930. A study of the mucosa of the genital tract of the cow, with special
410 reference to the cyclic changes. Am. J. Anat. 46, 261–301.

411 Crespo-Moral, M., García-Posadas, L., López-García, A., Diebold, Y., 2020. Histological
412 and immunohistochemical characterization of the porcine ocular surface. PLoS One 15,
413 e0227732.

414 Forchielli, M.L., Walker, W.A., 2005. The role of gut-associated lymphoid tissues and
415 mucosal defence. Br. J. Nutr. 93, S41–S48.

416 Hamada, H., Hiroi, T., Nishiyama, Y., Takahashi, H., Masunaga, Y., Hachimura, S.,
417 Kaminogawa, S., Takahashi-Iwanaga, H., Iwanaga, T., Kiyono, H., Yamamoto, H.,
418 Ishikawa, H., 2002. Identification of multiple isolated lymphoid follicles on the
419 antimesenteric wall of the mouse small intestine. J. Immunol. 168, 57–64.

420 Hammond, J., 1927. The physiology of reproduction in the cow. Nature 120, 37–39.

421 Hellings, P., Jorissen, M., Ceuppens, J., 2000. The Waldeyer's ring. Acta Otorhinolaryngol.

422 Belg. 54, 237–241.

423 Hickey, D.K., Patel, M. V., Fahey, J. V., Wira, C.R., 2011. Innate and adaptive immunity at
424 mucosal surfaces of the female reproductive tract: Stratification and integration of
425 immune protection against the transmission of sexually transmitted infections. J.
426 Reprod. Immunol. 88, 185–194.

427 Hunt, J.S., 1994. Immunologically relevant cells in the uterus. Biol. Reprod. 50, 461–466.

428 Jericho, K.W.F., Derbyshire, J.B., Jones, J.E.T., 1971. Intrapulmonary lymphoid tissue of
429 pigs exposed to aerosols of haemolytic streptococcus group L and porcine adenovirus.
430 J. Comp. Pathol. 81, 1–11.

431 Kathrine, E., Steen, J., 2011. A review of the human vs. porcine female genital tract and
432 associated immune system in the perspective of using minipigs as a model of human
433 genital Chlamydia infection. Vet. Res. 46, 1–13.

434 Kenneth Murphy, C.W., 2017. Janeway's Immunobiology - 9th Edition. Garland Science,
435 Taylor & Francis Group, New York.

436 Knop, E., Knop, N., 2011. The eye-associated lymphoid tissue (EALT) - A basis of the
437 anatomy and immunology at the ocular surface. Acta Ophthalmol. 89, 0–0.

438 Komban, R.J., Strömberg, A., Biram, A., Cervin, J., Lebrero-Fernández, C., Mabbott, N.,
439 Yrlid, U., Shulman, Z., Bemark, M., Lycke, N., 2019. Activated Peyer′s patch B cells
440 sample antigen directly from M cells in the subepithelial dome. Nat. Commun. 10,
441 1–15.

442 Konig, H., Liebich, H., 2007. Veterinary anatomy of domestic mammals: Textbook and
443 colour atlas, 3rd ed. Schattauer, New York.

444 Kracke, A., Hiller, A.S., Tschernig, H., Kasper, M., Kleemann, W.J., Troger, H.D., Pabst,
445 R., 1997. Larynx-associated lymphoid tissue (LALT) in young children. Anat. Rec.
446 248, 413–420.

447 Kuper, C.F., Koornstra, P.J., Hameleers, D.M.H., Biewenga, J., Spit, B.J., Duijvestijn,
448 A.M., Van Breda Vriesman, P.J.C., Sminia, T., 1992. The role of nasopharyngeal
449 lymphoid tissue. Immunol. Today 12, 219–224.

450 Lanzkowsky, P., Lipton, J.M., Fish, J.D., 2016. Lanzkowsky's Manual of Pediatric
451 Hematology and Oncology, Sixth Edition. Academic Press.

452 Lehner, T., Panagiotidi, C., Bergmeier, L.A., Tao, L., Brookes, R., Gearing, A., Adams, S.,
453 1995. Genital-associated lymphoid tissue in female non-human primates. Adv. Exp.
454 Med. Biol. 371, 357–365.

455 Liebler-Tenorio, E., Pabst, R., Liebler, E., Liebler-tenorio, E.M., 2006. MALT structure
456 and function in farm animals. Vet. Res. 37, 257–280.

457 Mair, K.H., Sedlak, C., Käser, T., Pasternak, A., Levast, B., Gerner, W., Saalmüller, A.,
458 Summerfield, A., Gerdts, V., Wilson, H.L., Meurens, F., 2014. The porcine innate
459 immune system: An update. Dev. Comp. Immunol. 45, 321–343.

460 Manesse, M., Delverdier, M., Abella-Bourges, N., Sautet, J., Cabanié, P., Schelcher, F.,
461 1998. An immunohistochemical study of bovine palatine and pharyngeal tonsils at 21,

462 60 and 300 days of age. Anat. Histol. Embryol. 27, 179–185.

463 Moyron-Quiroz, J.E., Rangel-Moreno, J., Kusser, K., Hartson, L., Sprague, F., Goodrich, S.,
464 Woodland, D.L., Lund, F.E., Randall, T.D., 2004. Role of inducible bronchus
465 associated lymphoid tissue (iBALT) in respiratory immunity. Nat. Med. 10, 927–934.

466 Nair, P.N.R., Schroeder, H.E., 1986. Duct-associated lymphoid tissue (DALT) of minor
467 salivary glands and mucosal immunity. Immunology 57, 171–17180.

468 Ochiel, D., Fahey, J., Ghosh, M., Haddad, S., Wira, C., 2008. Innate immunity in the
469 female reproductive tract: Role of sex hormones in regulating uterine epithelial cell
470 protection against pathogens. Curr. Womens. Health Rev. 4, 102–117.

471 Owen, R., Jones, A., 1974. Epithelial cell specialization within human Peyer's patches: an
472 ultrastructural study of intestinal lymphoid follicles. Gastroenterology 66, 189–203.

473 Parsons, K.R., Howard, C.J., Jones, B. V, Sopp, P., 1989. Investigation of bovine gut
474 associated lymphoid tissue (GALT) using monoclonal antibodies against bovine
475 lymphocytes. Vet. Pathol. 26, 396–408.

476 Pollard, M., Sharon, N., 1970. Responses of the Peyer's patches in germ-free mice to
477 antigenic stimulation. Infect. Immun. 2, 96–100.

478 Randall, T.D., 2010. Bronchus-associated lymphoid tissue (BALT). Structure and function.
479 Adv. Immunol. 107, 187–241.

480 Russell, M.W., Mestecky, J., 2002. Humoral immune responses to microbial infections in
481 the genital tract. Microbes Infect. 4, 667–677.

Schneider, P., Takatsuka, H., Wilson, A., Mackay, F., Tardivel, A., Lens, S., Cachero, T.G., Finke, D., Beermann, F., Tschopp, J., 2001. Maturation of marginal zone and follicular B cells requires B cell activating factor of the tumor necrosis factor family and is independent of B cell maturation antigen. J. Exp. Med. 194, 1691–1697.

Silva, F.M.O., Guimarães, J.P., Vergara-Parente, J.E., Carvalho, V.L., Carolina, A., Meirelles, O., Marmontel, M., Oliveira, B.S.S.P., Santos, S.M., Becegato, E.Z., Evangelista, J.S.A.M., Miglino, M.A., 2016. Morphology of mucosa-associated lymphoid tissue in odontocetes. Microsc. Res. Tech. 79, 845–855.

Tommola, P., Bützow, R., Unkila-Kallio, L., Paavonen, J., Meri, S., 2015. Activation of vestibule-associated lymphoid tissue in localized provoked vulvodynia. Am. J. Obstet. Gynecol. 212, 476.e1-476.e8.

Wang, J., Gusti, V., Saraswati, A., Lo, D.D., 2011. Convergent and divergent development among M cell lineages in mouse mucosal epithelium. J. Immunol. 187, 5277–5285.

Wang, Y., Sui, Y., Kato, S., Hogg, A.E., Steel, J.C., Morris, J.C., Berzofsky, J.A., 2015. Vaginal type-II mucosa is an inductive site for primary CD8+ T-cell mucosal immunity. Nat. Commun. 6, 1–13.

Wojciech, P., Ross, M.H., 2020. Histology: A text and atlas: with correlated cell and molecular biology, 8th ed. Wolters Kluwer, Philadelphia.

Zhang, J., Kuolee, R., Patel, G., Chen, W., 2007. Intestinal M cells: the fallible sentinels? World J. Gastroenterol. 13, 1477–1486.

Figure legends

Figure 1. Distribution of GOALTs in the mucosa of the VV and EPGOs of cows.

(**A**) Gross anatomical features of the VV and EPGOs with whole-mount staining using hematoxylin. White and red asterisks indicate the external urethral orifice and clitoris, respectively. One scale of the ruler is 1 mm.

(**B**) Magnified image of the VV mucosa squared area in panel A. Scale bars = 1 cm.

(**C**) Magnified image of the EPGO mucosa squared area in panel A.

Black arrowheads indicate hematoxylin-positive spots. Scale bars = 1 mm.

(**D**) Histology of hematoxylin-positive spot squared area in panel B. Histological observation revealed the spot is a cell aggregation, the GOALT, part of genital lymphoid ring. H&E staining. Scale bar = 100 μm.

(**E**) Schematic illustration of cutaway of the VV and EPGO area, including the vulva and clitoris. For morphometry, the mucosal area is divided into six regions. Blue circles indicate GOALTs.

(**F**) The density of GOALTs in the VV mucosa (number/cm^2).

Values = mean ± SE. n = 8.

GOALT: genital organ-associated lymphoid tissue, VV: vaginal vestibule, EPGOs: external parts of genital organs, H&E: hematoxylin & eosin

Figure 2. Histological characteristics of GOALTs in the cow VV.

(**A**) Isolated-type LF. LF localizes in the deep portion of the lamina propria and is fully surrounded by connective tissues.

(**B**) Migrating-type LF. Scattered lymphocytes are observed between LF and VV epithelium.

(**C**) Bordering-type LF. LF directly faces the VV lumen, and the VV epithelium is occupied by lymphocytes.

(**D**) Double migrating-type LF.

Dotted lines indicate the border of LFs. H&E staining. Scale bars = 100 μm.

(**E**) Triangle-type DLT.

(**F**) C-shaped-type DLT.

(**G**) Amorphous-type DLT. Dotted lines indicate the border of the DLT.

(**H**) Oval-type DLT.

Scale bars = 100 μm.

(**I**) Appearance of the percentage of LFs and DLTs in the examined GOALTs of the VV. $n = 8$.

(**J**) Appearance of the percentage of each type of LF in the examined LFs of the VV. $n = 8$.

(**K**) Appearance of the percentage of each type of DLT in the examined DLTs of the VV. $n = 8$.

GOALT: genital organ-associated lymphoid tissue, VV: vaginal vestibule, H&E: hematoxylin & eosin, LF: lymphatic follicle, DLT: diffuse lymphoid tissue

Figure 3. Immune cells composing the LF-type GOALT in the cow VV.

IHC was performed in the VV mucosa, and immune cells and high endothelial venules were found in the GOALTs.

(**A**) CD20 for B-cells.

(**B**) CD3 for T-cells.

(**C**) IBA1 for macrophages.

(**D**) MHCII for APCs.

(**E**) PNAd for high endothelial venules.

Squares denote the magnified area. Black arrowheads indicate positive cells for the IHC. Scale bars = 100 and 25 μm (low and high magnifications, respectively).

(**F**) Percentage of each examined cell occupying the LF. Values = mean ± SE. $n \geq 4$.

Significant differences between the immune cells indicated by ∗, $P < 0.01$; Kruskal–Wallis test followed by the Scheffé method.

GOALT: genital organ-associated lymphoid tissue, VV: vaginal vestibule, LF: lymphatic follicle, IHC: immunohistochemistry, APCs: antigen-presenting cells

Figure 4. Immune cells composing the DLT-type GOALT in the cow VV.

IHC was performed in the VV mucosa, and immune cells and high endothelial venules were found in the GOALTs.

(**A**) CD20 for B-cells.

(**B**) CD3 for T-cells.

(**C**) IBA1 for macrophages.

(**D**) MHCII for APCs.

(**E**) PNAd for high endothelial venules.

Black arrowheads indicate positive cells for the IHC. Scale bars = 100 μm.

(**F**) Percentage of each examined cell occupying the DLT. Values = mean ± SE. $n \geq 4$. Significant differences between the immune cells indicated by ∗, $P < 0.01$; Kruskal–Wallis test followed by the Scheffé method.

GOALT: genital organ-associated lymphoid tissue, VV: vaginal vestibule, DLT: diffuse lymphoid tissue, IHC: immunohistochemistry, APCs: antigen-presenting cells

Figure 5. Epithelium covering and connective tissue fibers composing the GOALTs in the cow VV.

(**A, B**) Amorphous-type DLT. Destroyed epithelium located between DLT and intralumenal area. The square indicates the magnified area. Red arrows denote peeled-off area of epithelial cells. H&E staining. Scale bars = 100 μm.

(**C, D**) Mucosal epithelium features stained using IHC for occludin. Panel C shows the epithelium that does not cover the LT. Panel D shows the epithelium covering the LT. Black arrowheads indicate positive reaction for the occludin. Scale bars = 50 μm.

(**E**) Connective tissue fibers of LF and DLT stained using PSR under polarized conditions. White dotted line indicates the border between the lamia propria and the epithelium. Blue dotted line denotes the border of the LF. Lower panel is a magnification of the squared area in the upper panel.

(**F, G**) Mucosal epithelium and connective tissue fibers stained using PSR. Panel F shows the mucosa with epithelium that does not cover the DLT. Panel G shows the mucosa with

589 epithelium covering the DLT. Upper and lower panels show optimal and polarized
590 conditions, respectively. Black and white dotted lines indicate the border between the lamia
591 propria and the epithelium.
592 Scale bars = 100 μm.
593 GOALT: genital organ-associated lymphoid tissue, VV: vaginal vestibule, DLT: diffuse
594 lymphoid tissue, IHC: immunohistochemistry, H&E: hematoxylin & eosin, LF: lymphatic
595 follicle, LT: lymphoid tissue, PSR: picrosirius red

Figure 6. Ultrastructure of mucosal epithelium covering the GOALT of the cow VV.

(**A**) VV mucosa stained in whole-mount with hematoxylin. GOALTs can be observed as hematoxylin-positive spots. Scale bars = 1 mm.

(**B**) VV mucosa examined using SEM. The same area as in panel A was examined. Scale bars = 100 μm.

White arrow heads indicate GOALTs.

(**C, D**) High-magnified areas squared in panel B. Black arrow heads indicate migrating lymphocytes from the GOALT to the lumen of the VV. Red arrow represents small protrusions that could be lymphocytes. Scale bars = 10 μm.

(**E**) VV mucosa on large GOALTs examined using SEM. Red arrow represents small protrusions that could be lymphocytes. Scale bars = 100 μm.

(**F**) High-magnified area of panel E. High-magnified areas squared in panel E. Black arrowhead indicates lymphocytes. Scale bars =10 μm.

(**G**) High-magnified area of panel F. High-magnified areas squared in panel F. Yellow arrowhead indicates erythrocytes. Scale bars = 2 μm.

GOALT: genital organ-associated lymphoid tissue, VV: vaginal vestibule, SEM: scanning electron microscopy

Figure 7. Schematic illustration of GOALTs in the mucosa of the VV and EPGOs in cows.

GOALTs consist of various shaped LFs and DLTs that localize in different regions in the lamina propria of the VV. Both LTs contain B-cells, T-cells, macrophages, and APCs. B-cells are dominant. Germinal centers are frequently observed in the center of the LF. High endothelial venules also appeared between LTs and surrounding connective tissues in the lamina propria. Moreover, collagenous fibers are stretched across the lamina propria, whereas reticular fibers are mainly observed in DLTs rather than in LFs. Characteristically, the epithelium covering GOALTs is partially or completely disrupted by the invasion of immune cells composing LFs and DLTs. These GOALTs are arranged as ring in the VV and EPGO mucosa and named the “genital lymphoid ring.”

GOALT: genital organ-associated lymphoid tissue, VV: vaginal vestibule, DLT: diffuse lymphoid tissue, LF: lymphatic follicle, LT: lymphoid tissue, APCs: antigen-presenting cells, EPGOs: external parts of genital organs

Highlights

- Whole-mount staining revealed lymphoid tissues on the mucosa of vaginal vestibule
- Lymphoid tissues showed two types: lymphatic nodule or diffuse lymphoid tissue
- Disrupted epithelium allowed passage for immune cells into the intraluminal space

Declarations of competing interest

The authors declare that they have no known competing financial interest or personal relationships that could have influenced in any way the work reported in this paper.

Figure 1

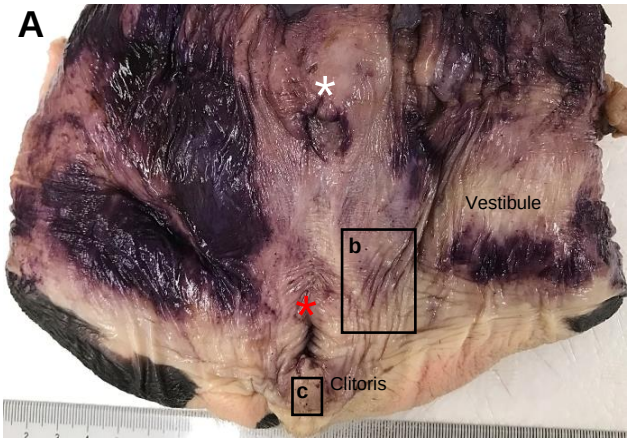
A
Vestibule
b
c
Clitoris

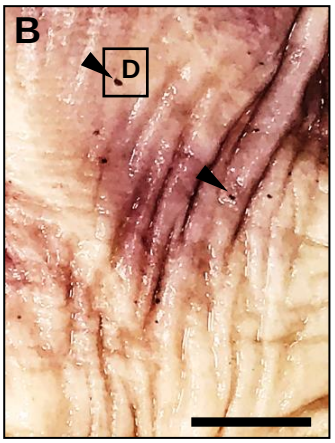
B
D

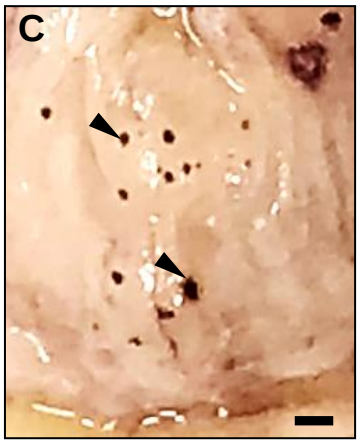
C

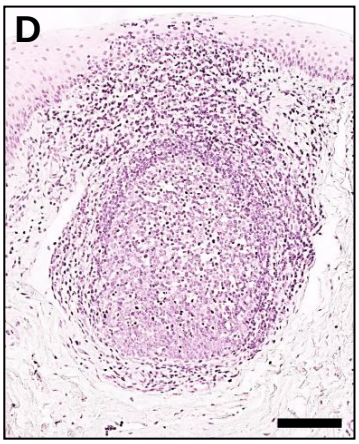
D

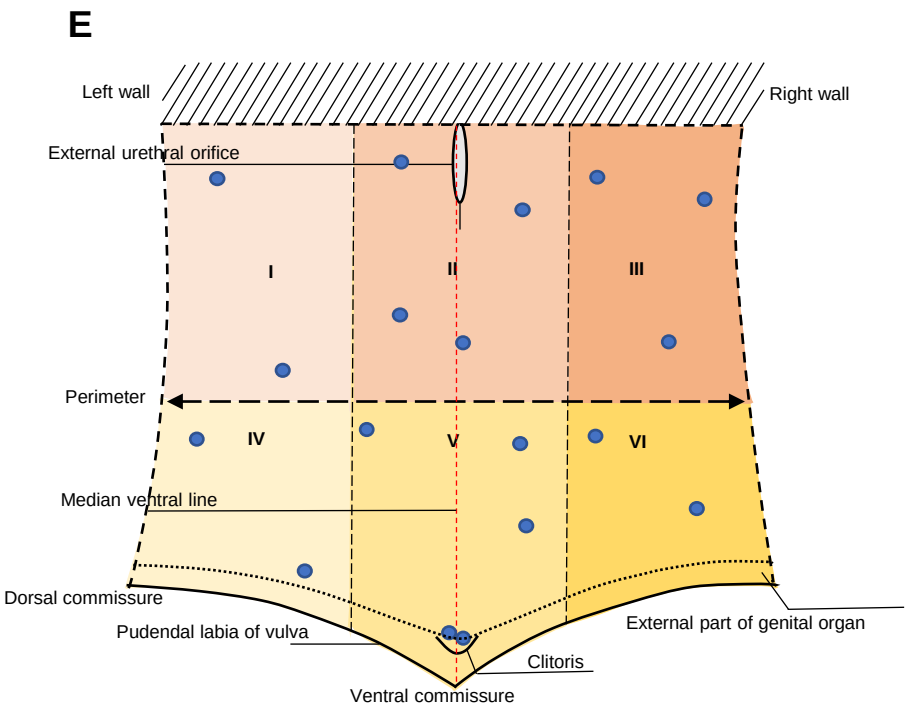
E
Left wall
Right wall
External urethral orifice
I
II
III
Perimeter
IV
V
VI
Median ventral line
Dorsal commissure
Pudendal labia of vulva
External part of genital organ
Clitoris
Ventral commissure

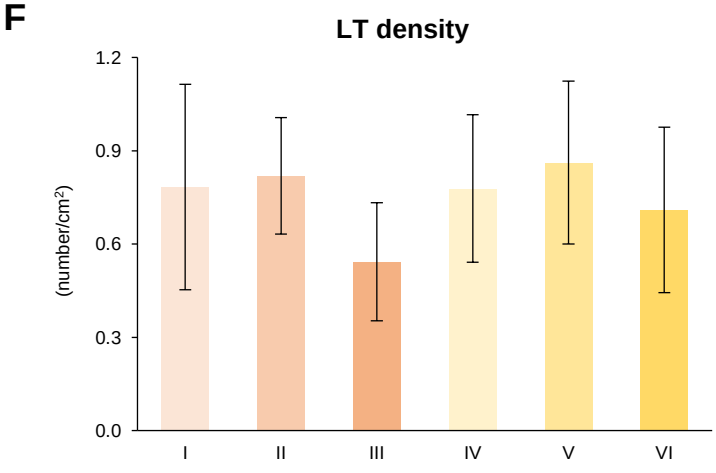
F
LT density
(number/cm²)
1.2
0.9
0.6
0.3
0.0
I
II
III
IV
V
VI

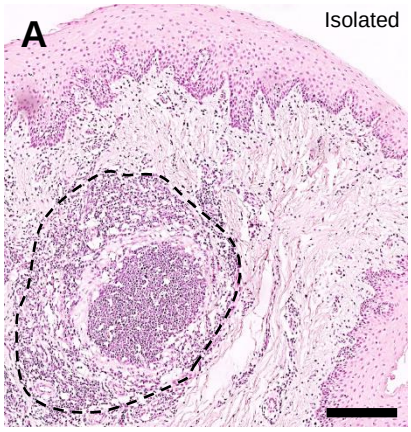
A
Isolated

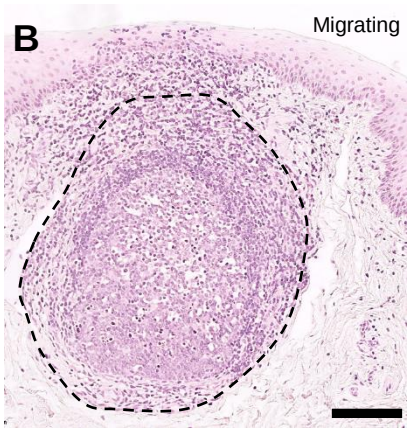
B
Migrating

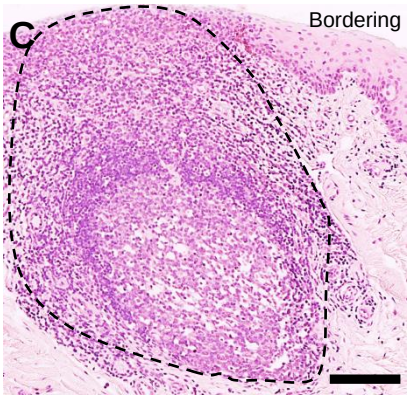
C
Bordering

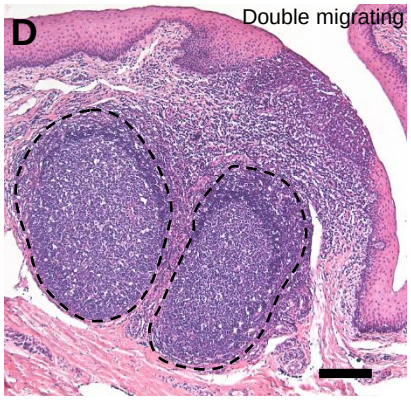
D
Double migrating

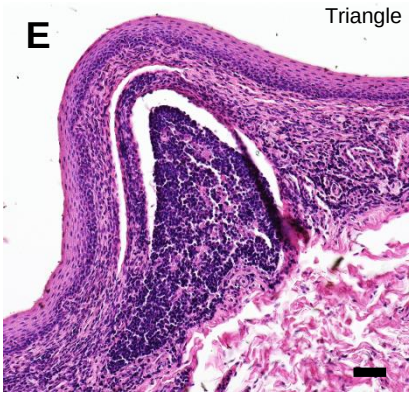
E
Triangle

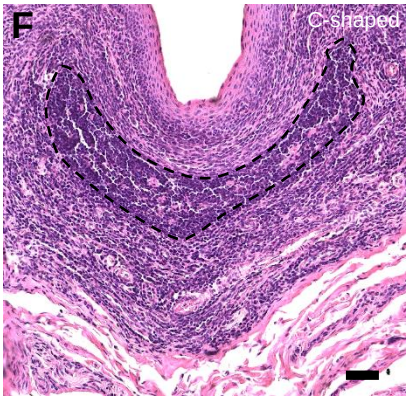
F
C-shaped

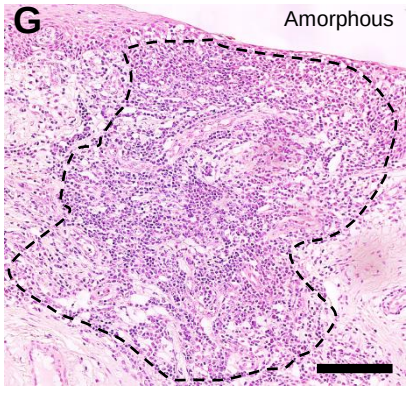
G
Amorphous

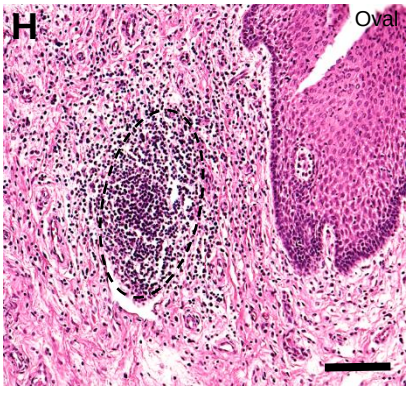
H
Oval

I

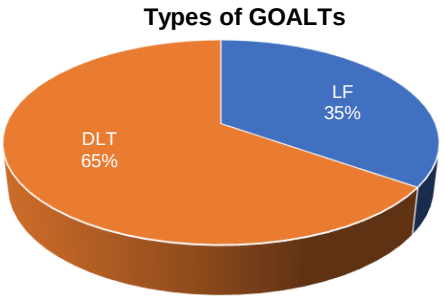
Types of GOALTs
LF
35%
DLT
65%

J

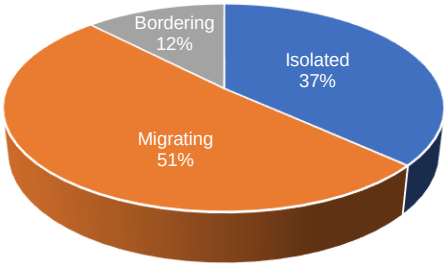
LF types
Bordering
12%
Isolated
37%
Migrating
51%

K

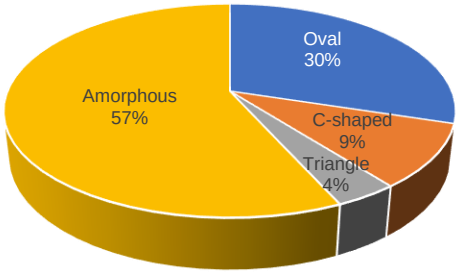
DLT types
Oval
30%
Amorphous
57%
C-shaped
9%
Triangle
4%

Figure 3

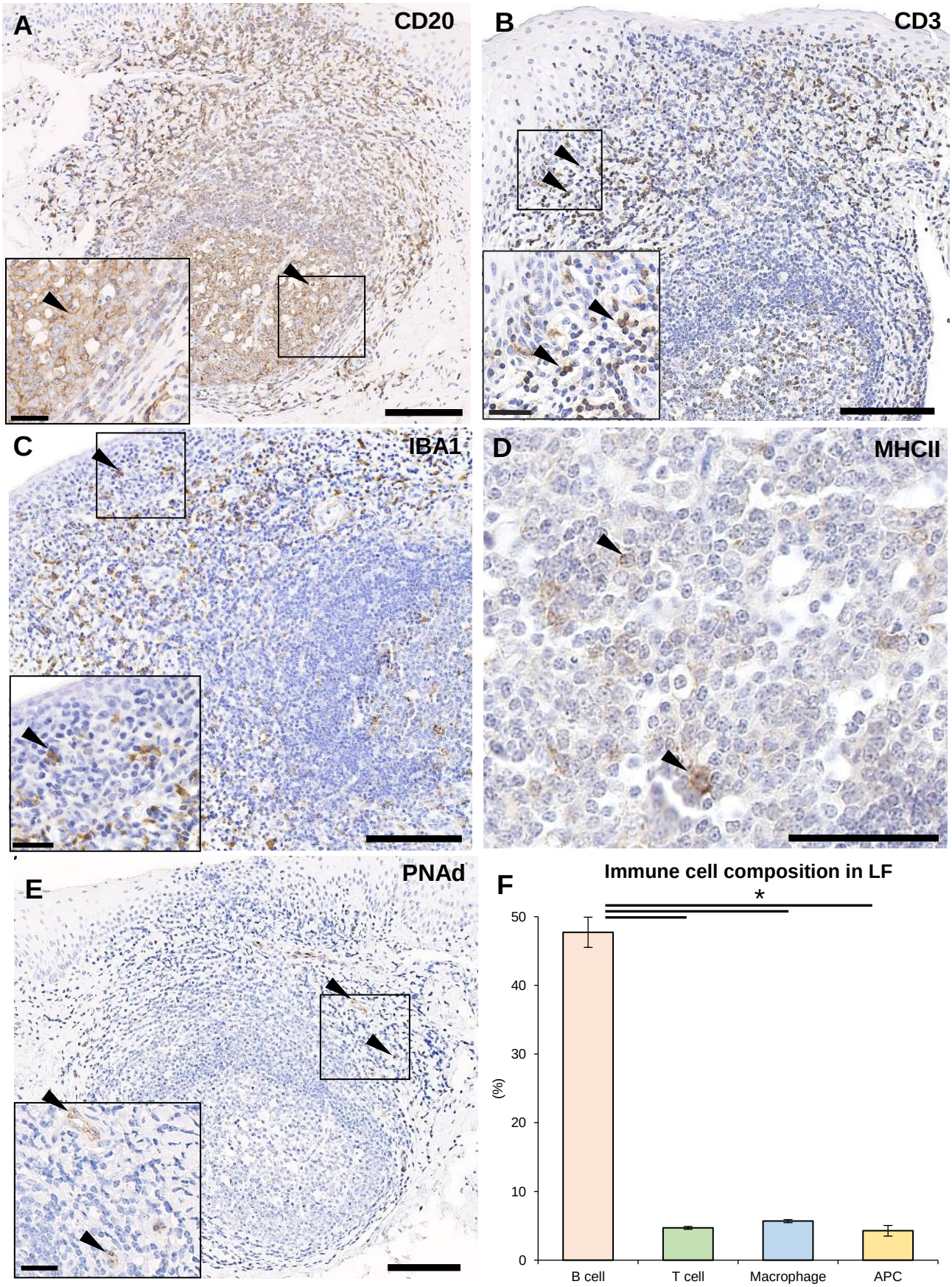
A
CD20
B
CD3
C
IBA1
D
MHCII
E
PNAd
F
Immune cell composition in LF
*
50
40
30
20
10
0
(%)
B cell
T cell
Macrophage
APC

Figure 4

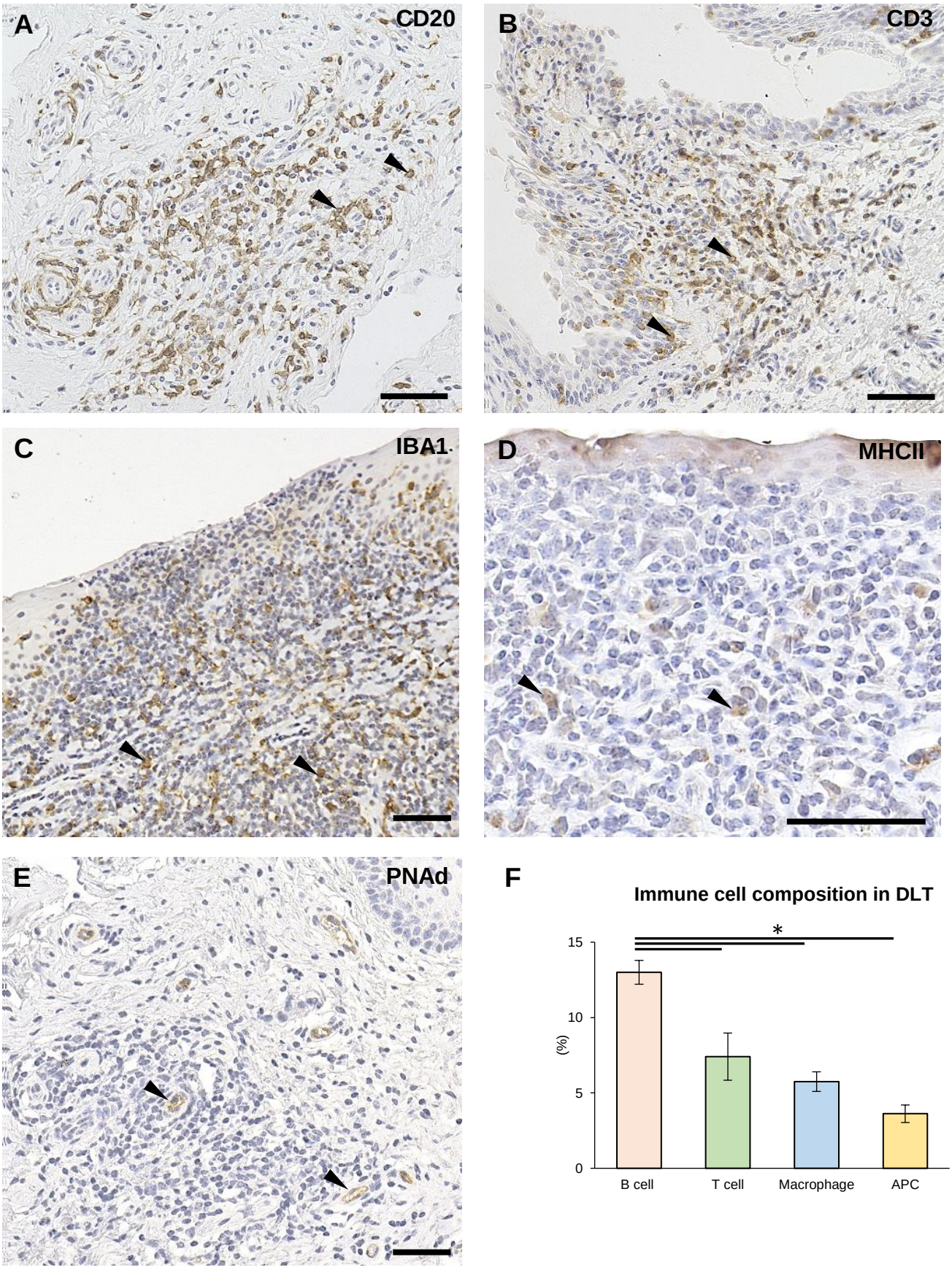
A
CD20
B
CD3
C
IBA1
D
MHCII
E
PNAd
F
Immune cell composition in DLT
*
15
10
5
0
(%)
B cell
T cell
Macrophage
APC

Figure 5

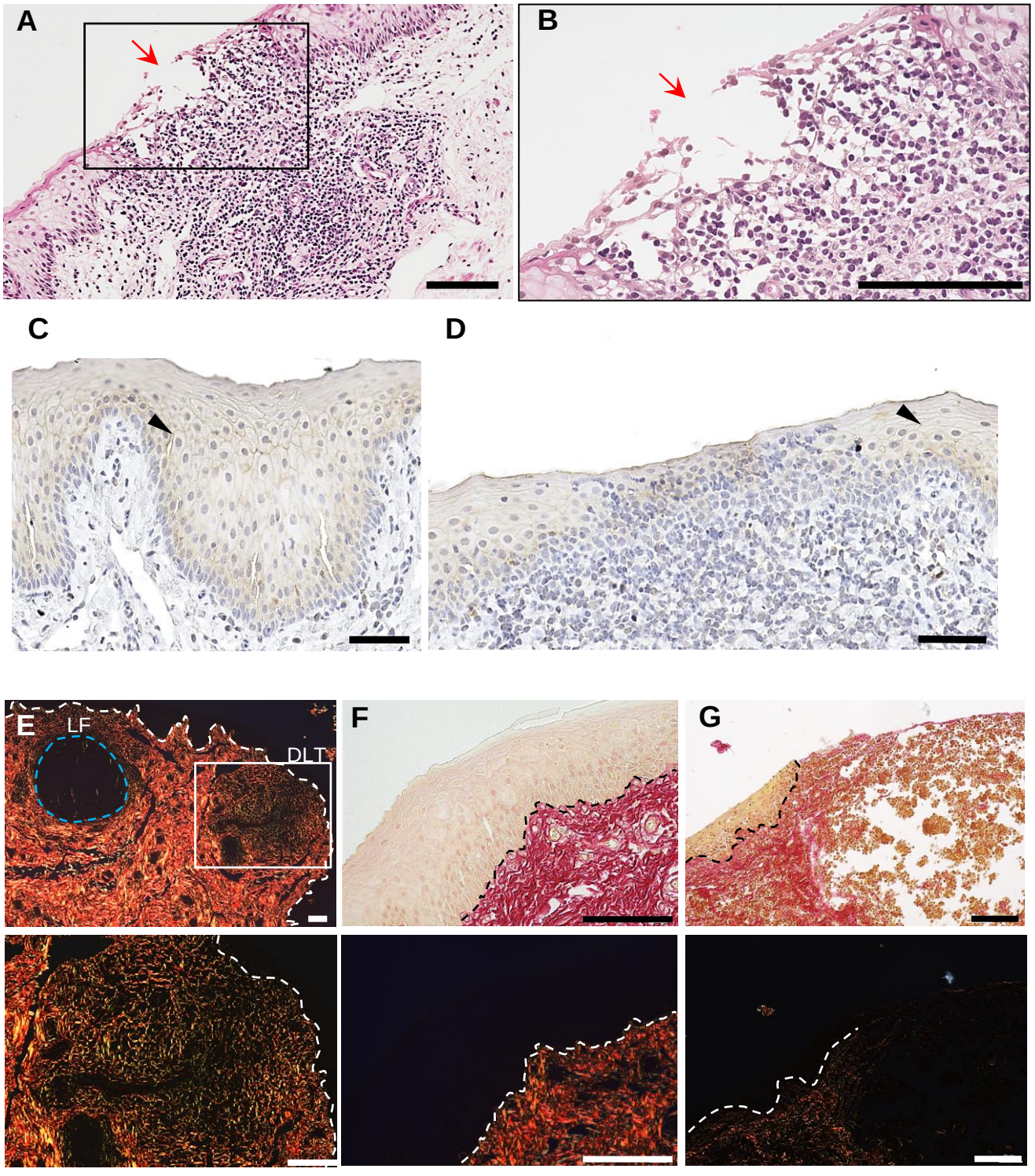

Figure 6

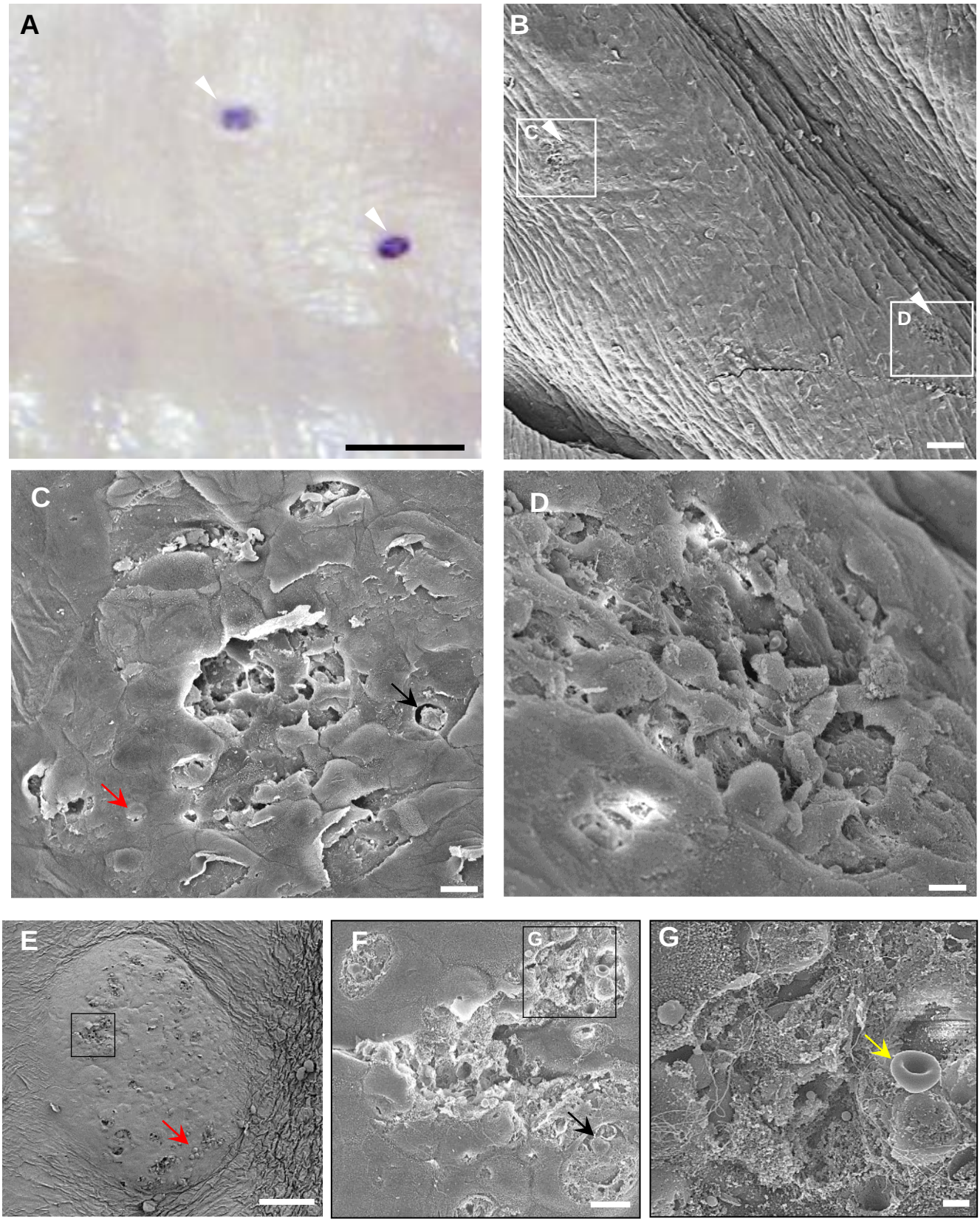

Figure 7

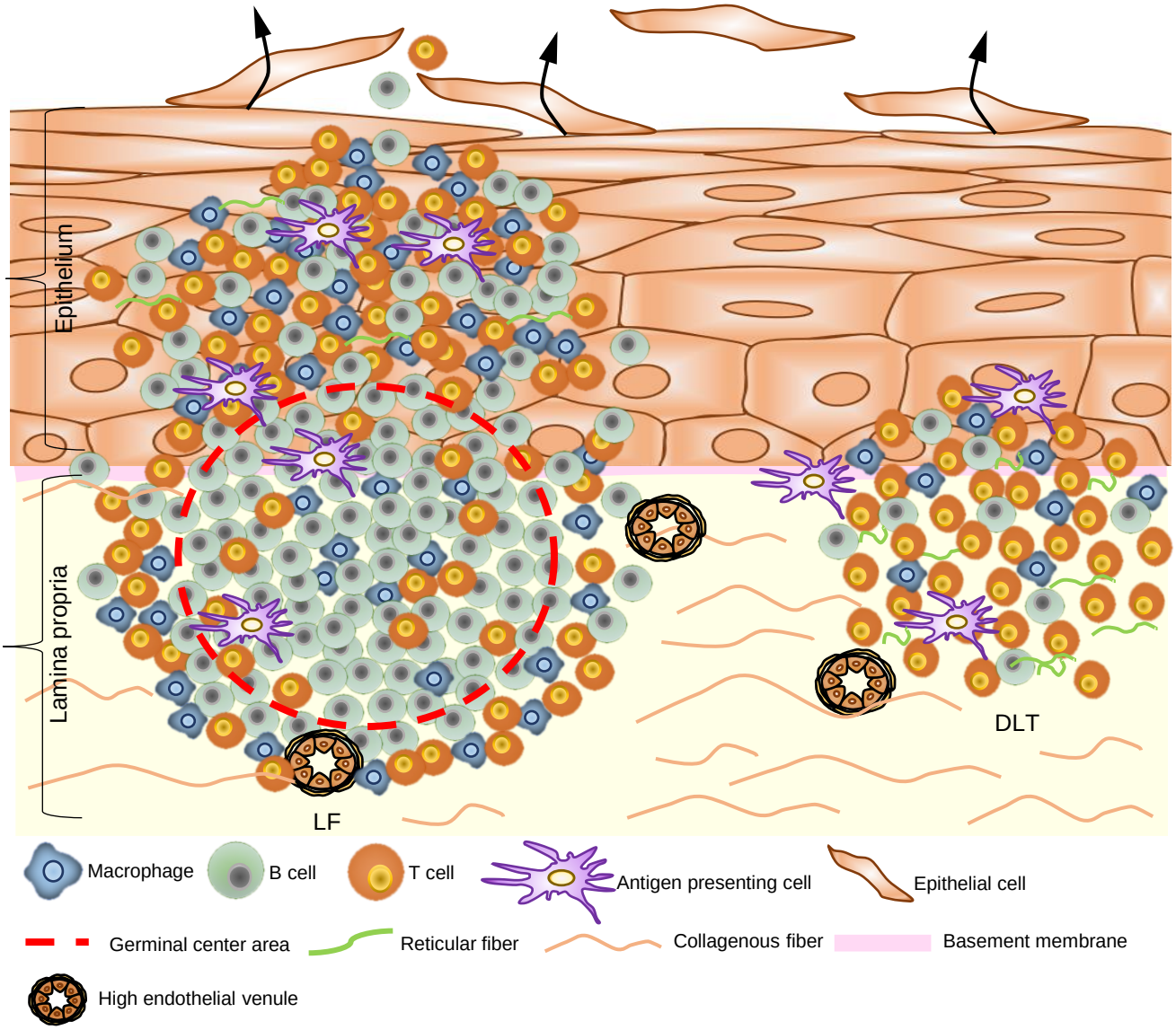
Epithelium
Lamina propria
LF
DLT
Macrophage
B cell
T cell
Antigen presenting cell
Epithelial cell
Germinal center area
Reticular fiber
Collagenous fiber
Basement membrane
High endothelial venule